

Supporting Information

High-resolution temperature-concentration diagram of α -synuclein conformation obtained from a single Förster resonance energy transfer image in a microfluidic device

Virginia Vandelinder[†], Allan Chris M. Ferreon[§], Yann Gambin[§], Ashok A. Deniz^{§*}, and Alex Groisman^{†*}

[†] *Department of Physics, University of California, San Diego, 9500 Gilman Dr., MC 0374, La Jolla CA, 92093*

[§] *Department of Molecular Biology, The Scripps Research Institute, 10550 N. Torrey Pines Road, 92037 La Jolla, CA*

Contents

Page 2-4: Design of the microfluidic device

Page 4-5: Fabrication of the microfluidic device

Page 5-6: Experimental set-up

Page 7-8: Supplementary Figure S1

Page 9: Supplementary Figure S2

* To whom correspondence should be addressed: agroisman@ucsd.edu, deniz@scripps.edu.

Design of the microfluidic device.

The gradient generator is designed according to principles described previously.¹ In the gradient generator, the source solutions, which are fed to the three inlets of the device, flow through a series of stages where they are repeatedly redistributed and mixed in different proportions (Figure 1 in the main text). The gradient generator contains four consecutive stages, each consisting of a single low-resistance redistribution channel (straight and long horizontal channels in Figure 1a-c in the main text) and a series of mixing channels (many of which have serpentine shapes) with widths $w_m = 25 \mu\text{m}$. The number of mixing channels in the k^{th} stage, N_k , is related to the number of mixing channel in the preceding stage, N_{k-1} , by a recurrence equation $N_k = 2N_{k-1} - 1$, and is nearly doubled between consecutive stages. The three channels connecting the device inlets to the redistribution channel of the 1st stage act as the 0th stage of the gradient generator with $N_0 = 3$. Hence, the number of separate mixing channels and solutions with different concentrations in the final (4th) stage of the generator is $N_4 = 33$. The device used in this study (Figure 1 in the main text) was designed to generate a linear series of concentrations from solutions with relative concentrations of 0, 50, and 100% fed to its three inlets.

The gradient generator is designed for mean flow velocities in a range of 20 – 40 $\mu\text{m/s}$ in each of the 8- μm -wide interrogation channels, corresponding to mean flow velocities of 0.45 – 0.9 mm/s in the central mixing channel of the 1st stage. The relatively low flow velocities (as compared with 6 mm/s in the 1st stage channels of the device in Ref. 1) and reduced channel width (25 μm vs. 50 μm in Ref. 1) substantially decreased the lengths of the mixing channels and of the footprint of the entire gradient generator. The reduced lengths of the mixing channels, especially in the 3rd and 4th stages, made it necessary to account for the finite flow resistance of the redistribution channels by adding segments with increased widths (and reduced resistance) at the entrances of every other mixing channels. The lengths and widths of the segments required to satisfy the equations of Ref. 1 were obtained from three-dimensional flow simulations in FEMLAB. The protein folding experiments were performed at a mean flow velocity of 30 $\mu\text{m/s}$ in the interrogation channels, corresponding to residence times $t_m \geq 2.25 \text{ s}$ for solutions flowing through the 25- μm -wide mixing channels. Therefore, the criterion for

complete mixing, $t_m \geq w_m^2 / D$,¹ was satisfied for diffusion coefficients $D > 2.8 \cdot 10^{-6}$ cm²/s. The mixing was expected to be complete for SDS (with $D \approx 10^{-5}$ cm²/s) and other small molecules, including fluorescein with $D \approx 5 \cdot 10^{-6}$ cm²/s. For micelles, which form at high concentrations of SDS and have D as low as $\sim 6 \cdot 10^{-7}$, numerical simulations indicated that the mixing in the 25- μ m-wide channels was expected to be 90% efficient (the non-uniformity of concentration, as measured by the coefficient of variance, is reduced to $\sim 10\%$ of its value at the mixing channel entrance).

The numbers of channels in the 0th and final (4th) stages in the present design are increased as compared with Ref. 1, 3 vs. 2 and 33 vs. 17, respectively. The use of 3 inlets, with a solution with an intermediate concentration fed to the central inlet, makes the operation of the gradient generator more robust and less sensitive to the imprecision of microfabrication. The streams coming from the 33 mixing channels of the 4th stage merge to create a flow with smooth linear concentration profile, which is then split between the 100 parallel interrogation channels. The extension of the merging area along the direction of flow, 40 μ m, is selected to allow sufficient diffusion time for smoothing of the steps in concentration between the streams (Figure 1c in the main text). The large number of the mixing channels leads to a small width of individual streams (50 μ m) that facilitates rapid smoothing without deterioration of the large-scale linear concentration profile. Such deterioration would occur if streams with different concentrations were allowed to flow side-by-side over a long distance.¹ To prevent this deterioration, the merging area is made short and the interrogation area is partitioned into an array of separate channels.

The fabrication procedure used to produce the 1 mm deep channels resulted in cross-sections of the hot and cold channels having a shape of an upside-down T, with a 1.2 mm wide, 0.1 mm tall rectangle at the bottom and a 1 mm wide, 0.9 mm tall rectangle at the top (Figure 1e in the main text and Figure S1a). The width and location of the bottom parts were defined lithographically with a high precision. The fabrication of the top 1 mm wide parts included a manual step, resulting in a somewhat lower precision (Figure S1a). Nevertheless, our two-dimensional (2D) numerical simulations of the heat transfer in the device indicated that the temperature gradient in the interrogation area had almost no sensitivity to the exact size of the top parts (Figure S1). The numerical simulations also indicated that the temperature profile in

the 1-mm-wide interrogation area is nearly perfectly linear (Figure S1d), with a range of temperatures of ~80% of the temperature difference between the cold and hot channels. (The high linearity and the reduced range of temperatures are both due to the 50 μm layer of PDMS between the circulation channels and the cover glass.) Finally, numerical simulations incorporating the effects of flow in the interrogation channels indicated that the perturbation of the temperature profile due to the flow is <0.25% of the temperature difference (<0.1 $^{\circ}\text{C}$ with the cold and hot channels at 15.5 and 53.5 $^{\circ}\text{C}$) for flow velocities <80 $\mu\text{m}/\text{s}$ (see Supporting Information, Figure S1). Thus, the flow of protein solutions at 30 $\mu\text{m}/\text{s}$ was expected to have a negligible effect on the temperature profile.

Fabrication of the microfluidic device.

Fabrication of the device required assembly of three layers of PDMS: a 50- μm -thick layer with flow channels, a 1-mm-thick layer with circulation channels, and a plain 4-mm-thick layer. The layers with flow and circulation channels were cast from two master molds that were fabricated using standard lithography techniques. The master mold for the flow layer was made by spin-coating an 8- μm -thick layer of UV-curable epoxy (SU8 2005, Microchem) onto a silicon wafer. The wafer was then exposed to UV light through a specially designed photomask (50,000 dpi, Fineline Imaging, Colorado Springs, CO) and developed. To create the master mold for the circulation layer, a 100- μm -thick layer of photoresist (SU8 2100) was spin-coated onto a different silicon wafer and then exposed to UV-light through a photomask. Another layer of photoresist, 15- μm -thick (SU8 2015), was spin-coated on top of the first layer and the wafer was exposed to UV-light through a different photomask (that was aligned with respect to the pattern in the 100- μm -thick layer) and developed.

To make the PDMS layer with circulation channels, a 1 mm thick layer of PDMS prepolymer (5:1 mixture of base and crosslinker of Sylgard 184, Dow Corning) was poured onto the circulation master mold and then baked in a 65 $^{\circ}\text{C}$ oven for 1 hour. The PDMS was then peeled off the mold and trimmed to the size of individual chips. The chips had 100 μm deep grooves for the bottom parts of the circulation channels. Straight segments of the grooves (0.6, 1.2, and 1.2-mm-wide for the room temperature, cold, and hot channels, respectively; Figure 1a) had additional 15 μm deep, 50 μm wide grooves in them that were parallel to and set back 100

μm from the edges of the 100 μm deep grooves. The 1 mm thick PDMS layer was cut all the way through by fitting a razor blade into the 15 μm deep grooves. In this manner, the cuts through the PDMS were straight, parallel, and precisely located 100 μm away from the lithographically fabricated channel edges, producing relatively well-defined T-shaped cross-sections of the circulation channels (Figure 1a and Supporting Information, Figure S1a). The cuts through the curved segments of the 100 μm deep grooves required lower precision and were made along the edges of the grooves.

The circulation layer chips were glued to plain, 4 mm thick slabs of PDMS using a very thin layer of PDMS, resulting in 5 mm thick monolith chips. Holes were punched through the chips to create access ports for the circulation channels. The master mold for the flow layer was spin-coated with a 50- μm -thick layer of PDMS (5:1 ratio of base to crosslinker). This layer was cured in an 80 °C oven for 15 minutes, to the point where the PDMS was solid but still tacky. Each 5 mm thick PDMS chip was then positioned with respect to the alignment marks on the flow layer. The assemblage was baked overnight in an 80 °C oven. The devices were then cut and peeled off of the flow layer master mold. Holes were punched for inlet and outlet ports to the flow layer. The PDMS devices were bonded to cover glasses by baking overnight in an 80 °C oven.

Experimental set-up

All solutions fed to flow layer inlets and drawn off from the outlet were kept in 500 μL Eppendorf tubes. The tubes were closed with PDMS plugs, with two small holes punched in each plug. To connect a tube to an inlet or outlet, a segment of a gauge-30 thin wall PTFE tubing (Cole Parmer, Vernon Hills, Illinois) was inserted through one of the holes in the plug to a position close to the bottom of the Eppendorf tube, and the other end of the segment was inserted into the device inlet or outlet. The other hole in the plug was used to vent the Eppendorf tube to atmosphere, while minimizing the evaporation of the liquid in it. The use of small Eppendorf tubes and the narrow PTFE tubing (inner diameter of 0.25 mm; internal volume of 1 μL per \sim 20 mm length) made it possible to perform experiments with small amounts of sample and buffers and to use the sample and buffers up to the last \sim 20 μL . The solutions in the Eppendorf tubes were centrifuged prior to use to prevent occasional

contaminating particles and debris from entering the PTFE tubing. This centrifugation was especially helpful when working with protein samples that were too small to filter. Flow through the flow layer channels of the device was driven by setting a differential hydrostatic pressure between the inlets and outlets that was controlled within ~5 Pa using vertical rails and sliding stages.¹

References

- (1) Campbell, K.; Groisman, A. *Lab on a Chip* **2007**, 7, 264-272.

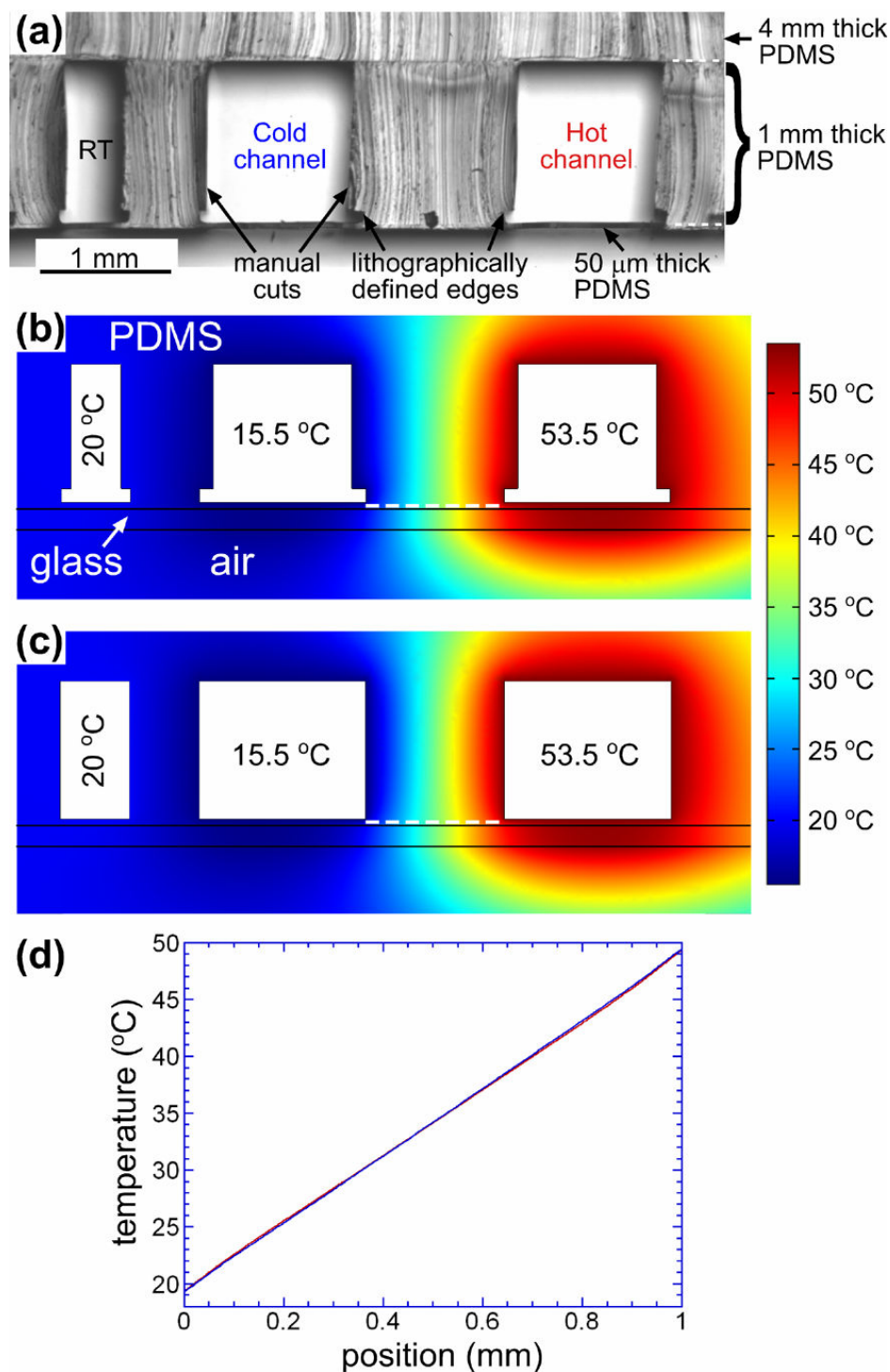


Figure S1. Temperature control in the microfluidic device.

(a) A Photograph of a cross-section of the microfluidic chip, showing the three water circulation channels, RT (room temperature), cold and hot, and the three-layer structure of the chip, with 50 μm bottom layer, 1 mm intermediate layer with 8 μm deep flow channels (not resolved), and 1 mm deep circulation channels. The circulation channels have shapes of upside-down T-s with the lower 0.1 mm deep parts (1.2 mm wide for the cold and hot channels) manufactured lithographically and the upper 0.9 mm deep parts cut manually.

(b)-(c) Fragments of cross-section of the microfluidic device, $\sim 5.5 \times 2$ mm in size, with a 0.6 mm layer of air beneath the cover glass with temperature distributions as obtained from steady state two-dimensional (2D) numerical simulations with FEMLAB. The computational domain of the simulations was 10 mm wide and consisted of 5 mm thick PDMS layer at the top with the circulation channels protruding into it by 1 mm from the bottom, a 50 μm thick PDMS layer below the 5 mm layer, a 0.15 mm layer of glass (cover glass) below the 50 μm thick PDMS, and a 1 mm layer of air at the bottom of the computational domain. The boundaries between PDMS, glass, and air, are shown by horizontal black lines. The thermal conductivities of PDMS, glass, and air, are taken as 0.15, 1.0, and 0.024 $\text{W}/\text{m}\cdot^\circ\text{C}$, respectively. The condition at all external boundaries of the computational domain is a temperature of 20 $^\circ\text{C}$ (room temperature). The conditions at the boundaries of the room temperature channel (left), cold channel (middle), and hot channel (right), are 20, 15.5, and 53.5 $^\circ\text{C}$, respectively, corresponding to the temperatures of water in the channels in the FRET experiment. White dashed lines above the glass surface mark the location of the interrogation channels, where the FRET measurements are taken. Panel (b) shows a temperature profile with the T-shaped channels that the device was designed to have (cf. panel (a)), whereas panel (c) shows a temperature profile with rectangular channels that have widths equal to those of the lower parts of the T-shaped channels in (b). To calculate the heat flow rate through the boundaries of the cold and hot circulation channels, the standard FEMLAB boundary integration function with the channel length (out-of-plane extension) of 12 mm was applied to the channels in (b), resulting in heat flow rates of 0.18 and 0.29 W, respectively.

(d) Distributions of temperature along the interrogation channels (dashed white lines) in the devices in (b) and (c) are shown by a red and blue curve, respectively. The temperature difference between the two curves does not exceed 0.2 $^\circ\text{C}$, indicating that the relatively low precision of the manual cuts, as seen in (a), has a minimal influence on the temperature profiles in the interrogation channels.

As a protein solution flows from left to right through an interrogation channel, its temperature increases to equilibrate with the local temperature of the channel walls. At sufficiently low flow velocity, the temperature profile in the channel remains linear, as in the case without flow shown in (d). Therefore, at a constant velocity along the channel (as required by the conservation of mass), there is a uniform rate of deposition of heat into the solution in the channel, and this rate is proportional to the flow velocity. Thus, in order to model the effect of the flow, we introduced a 1 mm wide 8 μm tall computational sub-domain at the actual location of the interrogation channels at the upper surface of the cover glass [white dashed line in (b)]. This computational sub-domain had a uniform negative heat production rate that was adjusted to obtain a 0.1 $^\circ\text{C}$ difference between the temperature profile with and without heat production [the latter case is the same as shown in (b) and (d)]. The heat production rate was found at an absolute value of $1.3 \cdot 10^7 \text{ J}/(\text{m}^3\cdot\text{s})$. For water, with a specific heat capacity of $4.2 \cdot 10^6 \text{ J}/(\text{m}^3\cdot^\circ\text{C})$, this heat production rate corresponds to a temperature change of 3 $^\circ\text{C}/\text{s}$. For a distance of 1 mm and a temperature difference of ~ 30 $^\circ\text{C}$ across the 1 mm length of interrogation channel, as in (d), this rate of temperature change corresponds to a flow velocity of 100 $\mu\text{m}/\text{s}$. At a flow velocity of 30 $\mu\text{m}/\text{s}$ in the interrogation channels, as in our FRET experiments, the perturbation to the temperature gradient due to the flow is expected not to exceed 0.03 $^\circ\text{C}$, which is negligible.

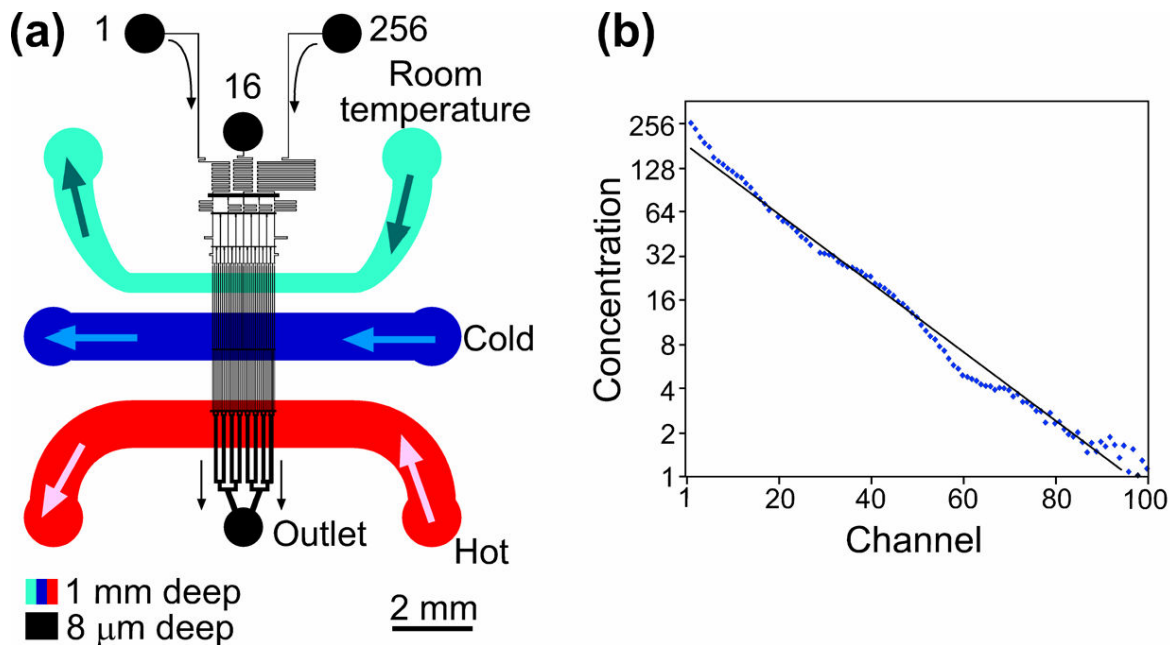


Figure S2. Microfluidic device designed to generate an exponential profile of concentrations and an orthogonal linear temperature gradient. **(a)** A schematic drawing of device. The flow channel network is shown in black. Three inlets of the flow layer are labeled by the relative concentrations of the solutions fed to them, 1, 16, and 256. The cyan, blue, and red channels (all 1 mm deep) are for circulation of room temperature, cold, and hot water, respectively. Arrows indicate flow directions. **(b)** Concentration of fluorescein (in relative units) in the interrogation channels (blue dots) as a function of channel number with 0.195, 3.125, and 50 ppm solution of fluorescein fed to the 1, 16, and 256 inlet, respectively. A concentration of 256 corresponds to the 50 ppm solution, and a concentration of 1 corresponds to the 0.195 ppm solution. Continuous black line corresponding to an exponential concentration profile is shown to guide the eye.